

Applications and Performance of HPC Resources for Parallel Analysis of Molecular Dynamics Trajectories with Python

Mahzad Khoshlessan

Tempe, Arizona, 85281

Elsevier Inc^{a,b}, Global Customer Service^{b,}*

^a*1600 John F Kennedy Boulevard, Philadelphia*

^b*360 Park Avenue South, New York*

Abstract

Typical size of the molecular dynamics (MD) trajectories from data-intensive bio-molecular simulations ranges from gigabytes to terabytes. However, the computational biophysics community misses effective use of high performance computing (HPC) resources for efficiently analyzing these trajectories and more importantly achieving linear scaling still remains a big challenge. Present work aims to provide insights, guidelines and strategies to the community on how to take advantage of the available HPC resources to gain the best possible performance. We investigated a single program multiple data (SPMD) execution model where each process executes the same program, to parallelize the Map-Reduce root mean square distance (RMSD) and Dihedral Featurization algorithms for analysis of MD trajectories in the MDAnalysis library. We employ the Python language because it is widely used in the bio-molecular simulation field and focus on an MPI-based implementation. We notice that straggler tasks negatively impact the performance and act as scalability bottlenecks. Straggler tasks are a very common problem in heterogeneous environments and

[☆]Fully documented templates are available in the elsarticle package on CTAN.

^{*}Corresponding author

Email address: support@elsevier.com (Global Customer Service)

URL: www.elsevier.com (Elsevier Inc)

¹Arizona State University.

are significantly slower than the mean execution time of all tasks, impeding job completion time. Our initial analysis shows that accessing a single file on the distributed file system leads to stragglers, and as a result, prevents any scaling beyond one node. We introduce an important performance parameter $t_{Compute}/t_{IO}$ which determines whether we observe any stragglers. In addition, we show that there are two factors that lead to stragglers including I/O and communication. Taking advantage of Global Arrays (GA) toolkit we have been able to obtain significant improvement in communication cost and performance. In addition, we show two different approaches to overcome the I/O bottleneck and compare their performance. First approach is splitting the trajectory into as many trajectory segments as number of processes. The second approach is through MPI-based approach using Parallel HDF5 where we examine the performance differences between both collective and independent I/O. Applying these strategies, we obtained near ideal scaling and performance.

Keywords: Python, MPI, HPC, MDAnalysis, Global Array, MPI I/O, Straggler, Molecular Dynamic

2010 MSC: 00-01, 99-00

1. Introduction

The increase in computational power coupled with sophisticated algorithms has lead rapid increase in the amount of data produced by MD simulations. Typical trajectory sizes from MD simulations range from gigabytes to terabytes. Therefore, analyzing these trajectories has become a very tedious process in many workflows and as a result people are trying to look for state of the art HPC tools (MPI and OpenMP) or Big Data ecosystem to tackle this problem. The need for parallel programming and running these programs on parallel architectures is obvious, however, efficiently programming for a parallel environment can be a very daunting task.

MDAnalysis [1, 2] is a widely used open-source Python library to analyze molecular dynamics (MD) simulations. *MDAnalysis* allows analysis of different

file formats for trajectories generated by various packages for molecular dynamic simulations.

15 In our previous study, we used a parallel map-reduce approach to study the performance of RMSD task [3]. We previously looked at the *Dask* library [4], which splits a computation in tasks and generates directed acyclic graphs (DAG) of these tasks that can be executed on a range of schedulers. We also implemented the parallel analysis scheme with MPI, using the *mpi4py* package [5, 6].
20 For both Dask and MPI we found that our benchmark task, the calculation of the minimum C_α RMSD for a subset of the residues in the enzyme adenylate kinase from a long MD simulation, only showed good strong scaling within a single node (up to 24 cores on *SDSC Comet*). However, with a single compute node we are limited by the resources for executing a given problem. Distributed
25 computing, allows parallelizing our problems for larger problem sizes and lead to performance gains. But, as soon as we extend the computation beyond a single node, performance drops due to *stragglers* tasks, a subset of Dask worker processes or MPI ranks that are significantly slower than the mean execution time of all tasks, increasing the total time to solution. Stragglers significantly
30 impede job completion time and are a big challenge toward achieving improved performance.

MPI should have, in principle, close to ideal scaling for a pleasingly parallel task such as the analysis of trajectory blocks, and does not require additional considerations of, e.g., scheduler performance as for Dask. Therefore, in the
35 present study, we analyze the MPI case in more detail to better understand the origin of the stragglers.

We want to provide simple and robust parallelization approaches to analyzing molecular dynamics (MD) trajectories, in order to remove a narrowing bottle neck in the bio-molecular simulation field. We have selected two of the most
40 common map-reduce algorithms in *MDAnalysis* one of which is I/O bound and the other is compute bound. We use SPMD paradigm to parallelize theses two algorithms on HPC resources. With SPMD, each process executes essentially the same code but on a different part of the data. We use Python, a machine-

independent, byte-code interpreted, object-oriented programming (OOP) language, which is well-established in HPC parallel environments [7]. Based on our initial analysis there is an important performance parameter, $t_{Compute}/t_{IO}$, that determines whether we observe stragglers. We show this behavior using RMSD and dihedral featurization algorithms. If $t_{Compute}/t_{IO} \gg 1$, the algorithm scales very well, otherwise it does not scale beyond one node. For the algorithms with small $t_{Compute}/t_{IO}$, we need to come up with strategies to improve scaling and overcome straggler problems. Looking at the timing distribution across all ranks we noticed that communication and I/O are the two main scalability bottlenecks. Taking advantage of Global Array toolkit [8], each rank places its data in shared memory which allows direct access using the global address space rather than through a message-passing protocol. This reduces communication cost noticeably. Although Global Array toolkit is very helpful for improving the performance it is still not enough because I/O remains a bottleneck. Our data shows that I/O time does not scale beyond one node. Due to the large file size and memory limit, processes are not able to load the whole trajectory into memory at once, and as a result each process is only allowed to load one frame into memory at a time. Therefore, with large number of frames, there will be a lot of file access requests and when the compute time is small with respect to I/O, then I/O can be a major issue. Hence, we needed to find ways to improve I/O scaling beyond a single compute node. In order to improve I/O scaling, we came up with two approaches: MPI-based approach using Parallel HDF5 [9], and splitting our trajectory to as many trajectory segments as the number of processes. We provide the detail on these approaches on the following sections. But, both approaches significantly improved the performance and we were able to achieve near ideal scaling.

70 2. Molecular Dynamics Analysis Applications

2.1. *MDAnalysis*

Simulation data exist in trajectories in the form of three dimensional time series (atoms positions and velocities), and these come in a plethora of different and idiosyncratic file formats. *MDAnalysis* is a widely used open source Python
75 library to analyze these trajectory files with an object oriented interface. The package is written in Python (compatible with version 2.7 and 3.4+), with time critical code in C/Cython.

2.1.1. *Root Mean Square Distance (RMSD)*

The calculation of the root mean square distance (**RMSD**) for C_{α} atoms
80 after optimal superposition with the QCPROT algorithm [10, 11] is commonly required in the analysis of molecular dynamics simulations (Algorithm 1). The task used for the purpose of our benchmark is the *MDAnalysis*.analysis.rms.rmsd() function from the *MDAnalysis*.analysis.rms module (implemented in Cython [1]). This function computes the RMSD between two sets
85 of coordinates using the fast QCPROT algorithm to optimally superimpose two structures and then calculates the RMSD.

To this, the protein structure (selected C_{α} atoms) in the initial frame will be considered as the reference and as the mobile group at other time steps. The superposition is done in the following way: First, the mobile group is translated
90 so that its center of mass coincides with the one of reference. Second, a rotation matrix is computed that spatially aligns the mobile group to reference which minimizes the RMSD between the coordinates of the mobile group and reference structure. Finally, all atoms in mobile group are shifted and rotated. For each frame, a non-negative floating point number is calculated and the final result
95 is a time-series of the RMSD. RMSD values show how rigid the domains in a protein structure are, during the transition. The order of complexity for RMSD algorithm 1 is $T \times N^2$ where T is the number of frames in the trajectory and N the number of particles in a frame.

Algorithm 1 RMSD Algorithm

Input: *mobile*: the desired atom groups to perform RMSD on them
bsize: Total number of frames assigned to each rank
xref0: mobile group in the initial frame which will be considered as reference
start & *stop*: that tell which block of trajectory (frames) is assigned to each rank
topology & *trajectory*: files to read the data structure from
Output: Calculated RMSD arrays

```

1: procedure Block_RMSD(index, topology, trajectory, xref0, start=None, stop=None,
   step=None)
2:   start00 = time.time()
3:   u = Universe(topology, trajectory)
4:   g = u.atoms[index]
5:
6:   start1 = time.time()
7:   start0 = start1
8:   for  $\forall$  iframe, ts in enumerate(u.trajectory[start : stop : step]) do
9:     start2 = time.time()
10:    results[iframe, :] = ts.time, MDAnalysis.analysis.rms.rmsd(g.positions,
   xref0, center=True, superposition=True)
11:    t.comp[iframe] = time.time()-start2                                ▷ Compute per frame
12:    t.IO[iframe] = start2-start1                                         ▷ I/O per frame
13:    start1 = time.time()
14:   end for
15:   start3 = time.time()
16:   return results
17: end procedure
18:
19: start4 = time.time()
20: mobile = Select C $\alpha$  atoms
21: index = indices of mobile atom group
22: xref0 = mobile.positions-mobile.center_of_mass()
23: out = Block_RMSD(index, topology, trajectory, xref0, start=start, stop=stop,
   step=1)
24:
25: start5 = time.time()
26: if rank == 0 then
27:   data1 = np.zeros([size*bsize,2], dtype=float)
28: else
29:   data1 = None
30:   comm.Gather(out[0], data1, root=0)
31: end if
32:
33: start6 = time.time()

```

2.1.2. Dihedral Featurization

100 As a real-world compute-bound task we investigated **Dihedral featuriza-**
tion [12] (Algorithm 2) whereby a time series of feature vectors consisting of the
two backbone dihedral angles per residue (ϕ_i and ψ_i) is calculated for all 212
non-terminal residues. For each frame, an array of dihedral angles is calculated
where for later convenience, an angle θ_i is actually represented as $(\cos \theta_i, \sin \theta_i)$.
105 The order of complexity for Dihedral featurization algorithm (Algorithm 2) is
 $T \times N$.

3. Background

3.1. MPI for Python *mpi4py*

MPI for Python (*mpi4py*) is a Python wrapper written over Message Passing Interface (MPI) standard and allows any Python program to employ multiple processors [5, 6]. Python has several advantages that makes it a very attractive language including rapid development of small scripts and code prototypes as well as large applications and highly portable and reusable modules and libraries. *Mpi4py*'s interface is designed to be as conforming as possible with standard MPI for C++, saving users from learning a new interface specification [7]. In addition, Python's interactive nature, and other factors like lines of codes (LOC), number of function invocation, and development time adds to its attractiveness and clarifies why it is a good investment to extend Python use to message-passing parallel programming applications. Based on the efficiency tests, the performance degradation due to using *mpi4py* is not prohibitive and the overhead introduced by *mpi4py* is far smaller than the overhead associated to the use of interpreted versus compiled languages [7]. In addition, there are works on improving the communication performance in *mpi4py* and it shows minimal overheads compared to C code if efficient raw memory buffers are used for communication [5].

3.2. Applications of Global Array

The classic message-passing paradigm of parallel programming not only transfers data but also synchronizes the sender and receiver. Asynchronous (nonblocking) send/receive operations can be used to avoid synchronization, but cooperation between sender and receiver is still required. The synchronization effect is beneficial in certain classes of algorithms, such as parallel linear algebra algorithms. However, for other algorithms, this synchronization can be unnecessary and undesirable, and a source of performance degradation and programming complexity. In the shared-memory programming model, data is located either in *private* memory which is accessible only by a specific process or in *global* memory which is accessible to all processes [8].

In shared-memory systems, regardless of the implementation, the shared-memory paradigm eliminates the synchronization that is required when message-passing is used to access shared data. A disadvantage of many shared-memory
140 models is that they do not expose the none-uniform memory access (*NUMA*) hierarchy of the underlying distributed-memory hardware.

Global array (GA) toolkit offers the best features of both shared and distributed programming models and allows manipulating physically distributed dense multi-dimensional arrays without the need for explicit cooperation by
145 other processes. The primary mechanisms provided by GA for accessing data are block copy operations that transfer data between layers of memory hierarchy, i.e. global memory (distributed array) and local memory. GA compliments message passing programming model and is compatible with MPI which allows the users to take advantage of existing MPI software/libraries [8].

150 The shared memory model based on Global Arrays combines the advantages of a distributed memory model with the ease of use of shared memory. This is achieved by function calls that provide information on which portion of the distributed data is held locally and the use of explicit calls to functions that transfer data between a shared address space and local storage. The combination of these functions allows users to make use of the fact that remote data
155 is slower to access than local data and to optimize data reuse and *minimize communication in their algorithms*.

The basic components of the Global Arrays toolkit are function calls to create global arrays (*ga_create*), copy data to (*ga_put*), from (*ga_get*), and between
160 global arrays (*ga_distribution*, *ga_scatter*), and identify and access the portions of the global array data that are held locally (*ga_access*). In addition, there are also functions to destroy arrays (*ga_destroy*) and free up the memory originally allocated to them [7].

Another study by [Thesis] extends GA to python through Numpy. This library is called Global Arrays in NumPy (GAiN). NumPy is inherently serial and
165 although NumPy's computational capabilities are efficient, it is still not enough for larger problem sizes. GAiN library attempts to extend the substantial work

in Global Arrays to large parallel array computation within the NumPy framework. This extension module to python provides users with access to global
170 arrays which makes GA implementation much easier and faster [7].

3.3. MPI and Parallel HDF5

MPI-based applications work by launching multiple parallel instances of the Python interpreter which communicate with each other via the MPI library. HDF5 itself handles nearly all the details involved with coordinating file access
175 through MPI library. This is advantageous to avoid multiple processes to compete over accessing the same file on disk. In fact in python, MPI-IO opens shared files with a mpio driver. In addition, MPI communicator should be supplied as well and the users also need to follow some constraints for data consistency [9].

3.3.1. Collective Versus Independent Operations

180 MPI has two flavors of operation: collective, which means that all processes have to participate in the same order, and independent, which means each process can perform the operation or not and the order also does not matter [9]. With HDF5, modifications to file metadata must be done collectively. In contrast, opening or closing a file, creating or deleting new datasets, groups,
185 attributes, or named types, changing a datasets shape, and moving or copying objects in the file or any type of data operations can be performed independently by processes. It should be noted that collective does not mean synchronized. Although in collective I/O all processes perform the same task, but they do not wait until the others catch up [9].

190 4. Method

The test system contained the protein adenylate kinase with 214 amino acid residues and 3341 atoms in total [13]. The trajectory was in Gromacs XTC format trajectory (“600x” in Khoshlessan et al. [3]) with a size of about 30 GB and 2,512,200 time frames (corresponding to $602.4 \sim \mu s$ simulated time)

195 which represents a typical medium per-frame size but is very long for current standards.

The experiments were executed on the XSEDE Supercomputers: *SDSC Comet*. SDSC Comet is a 2.7 PFlop/s cluster with 6,400 nodes in total. The standard compute nodes consist of Intel Xeon E5-2680v3 processors, 128 GB
 200 DDR4 DRAM (64 GB per socket), and 320 GB of SSD local scratch memory. The large memory nodes contain 1.5 TB of DRAM and four Haswell processors each and the network topology is 56 Gbps FDR Infini-Band. All the experiments in the present study are performed using compute nodes.

4.1. Timing observables

205 We model MPI performance based on the RMSD algorithm (1) and Dihedral Featurization algorithm (2). The notation for our models is summarized in Table 1. We directly measured inside our code (in the function `block_rmsd()`) the “compute” time per trajectory frame to perform the computation (`t_comp` in the code) and the “I/O” time for ingesting the data from the file system into
 210 memory, (`t_IO`). t_{comp_final} is the summation of “compute” time per frame and t_{IO_final} is the summation of “I/O” time per frame for all the frames assigned to each rank. t_{end_loop} is the time delay between the end of the last iteration and exiting the for loop. $t_{opening_trajectory}$ is the time which data structures are initialized and topology and trajectory files are opened.

215 Outside the `block_rmsd()` function, relevant probs were taken and stored as variables `start4`, `start5`, and `start6`, which we will abbreviate in the following as t_4 (after setting up the problem and before entering `block_rmsd()` to *ingest* and *compute*), t_5 , (before communicating back results with `MPI.COMM_WORLD.Gather()`), and t_6 (after all work has been done but
 220 before timing statistics are computed). The total time (for all frames) spent in `block_rmsd()` is $t_{RMSD} = t_5 - t_4$. The “Shuffle” time to gather (“reduce”) all data from all processor ranks is $t_{comm} = t_6 - t_5$.

There are parts of the code in `block_rmsd()` that are not covered by the detailed timing information of $t_{compute_final}$ and t_{I/O_final} . To measure the un-

Item	Definition
t_{end_loop}	$t_3 - t_1$
$t_{opening_trajectory}$	$t_0 - t_{00}$
t_{comp_final}	$sum(t_{comp})$
t_{IO_final}	$sum(t_{IO})$
t_{all_frame}	$t_3 - t_0$
t_{RMSD}	$t_5 - t_4$
$t_{Communication_{MPI}}$	$t_6 - t_5$
$t_{Communication_{GA}}$	$(t_6 - t_5) + (t_7 - t_6)$
$t_{Overhead1}$	$t_{all_frame} - t_{IO_final} - t_{comp_final} - t_{end_loop}$
$t_{Overhead2}$	$t_{RMSD} - t_{all_frame} - t_{opening_trajectory}$
t_N	$t_{RMSD} + t_{Communication}$
t_{total}	$\max t_N$

Table 1: Notation of our performance modeling (relevant probes in the codes are stored as variables `start*`, which we will abbreviate in here as t_*)

225 accounted time we define the “overheads”. $t_{Overhead1}$ and $t_{Overhead2}$ are the overhead of the calculations and they should be ideally very small. The total time to completion for a single process on N cores is t_N , which is mathematically equivalent to $t_N \equiv t_{RMSD} + t_{comm}$.

We also recorded the total time to solution $t_{total}(N)$ with N MPI processes
230 on N cores (which is effectively $t_{total}(N) \approx \max t_N$). Strong scaling was quantified by calculating the speed-up relative to performance on a single core (using MPI).

$$S = \frac{t_{total}(N)}{t_{total}(1)} \quad (1)$$

5. Performance Study

5.0.1. RMSD Benchmarks

235 RMSD algorithm for the present test case, represents a task for which computational workload per frame is smaller than I/O workload per frame ($t_{compute_per_frame} = 0.09$ ms, $t_{IO_per_frame} = 0.3$ ms, thus $t_{compute_final}/t_{IO_final} \approx 0.3$). We showed previously that the RMSD task only scaled well up to 24 cores,

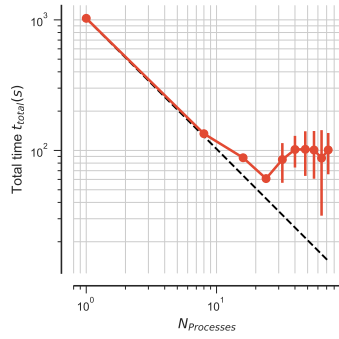
on a single compute node on *Comet* (and similarly also only on a single node
 240 on other machines), using either dask or MPI [3]. Although, it is not clear that
 the root cause is the same for dask and MPI, here we focus on the MPI imple-
 mentation (via *mpi4py* [5, 6]) for its greater simplicity than dask, in order to
 better understand the cause for the poor scaling across nodes.

For both dask and MPI we observed stragglers, individual workers or MPI
 245 ranks, that take much longer to complete than mean execution time of all other
 workers or ranks. Waiting for these stragglers destroys strong scaling perfor-
 mance, as shown in Figure 1a, 1b for MPI.

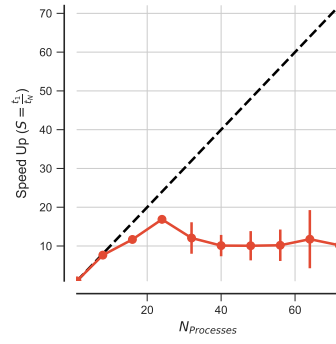
In the example run in Figure 1c, ten ranks out of 72 take almost 65 s whereas
 the remaining ranks only take about 40 s. The detailed breakdown of the time
 250 spent on each rank (Figure 1c) shows that time for the actual computation,
 $t_{\text{compute_final}}$, is fairly constant across ranks. The time spent on reading data
 from the shared trajectory file on the Lustre file system into memory, $t_{\text{I/O_final}}$,
 shows variability across different ranks. Stragglers, however, appear to be de-
 fined by occasional much larger *communication* times, t_{comm} (lines 25-30 in 1),
 255 that are on the order of 30 s in this example. For other ranks, t_{comm} varies
 across different ranks and for a few ranks $t_{\text{comm}} < 10$ s or is barely measur-
 able. This initial analysis (especially Figure 1c) indicates that communication
 is a major issue.

Identification of Scalability Bottleneck

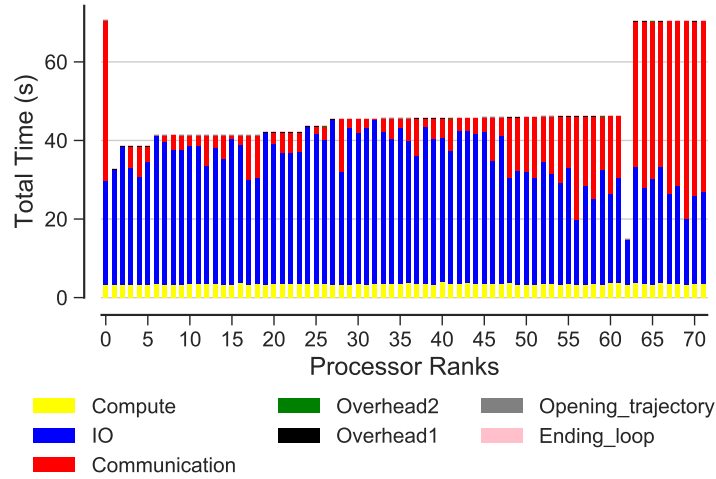
260 Figure 2 shows the scaling of $t_{\text{compute_final}}$ and $t_{\text{I/O_final}}$ individually. As
 shown, $t_{\text{compute_final}}$ scales very well; however, $t_{\text{I/O_final}}$ does not show good
 scaling beyond a single node (24 cores) and that explains why we are seeing
 these variations in $t_{\text{I/O_final}}$ across different ranks (Figure 1c). Considering the
 results in Figures 1 and 2, we can conclude that communication and I/O are
 265 the root causes for stragglers.



(a) Scaling total



(b) Speed-up



(c) Compute $t_{\text{compute_final}}$, IO $t_{\text{I/O_final}}$, communication t_{comm} , ending the for loop $t_{\text{end_loop}}$, opening the trajectory $t_{\text{opening_trajectory}}$, and overheads $t_{\text{Overhead1}}$, $t_{\text{Overhead2}}$ per MPI rank (as described in methods).

Figure 1: Performance of the RMSD task with MPI which is I/O-bound $t_{\text{compute_final}}/t_{\text{I/O_final}} \approx 0.3$. Data are read from the file system (I/O included) and results are communicated back to rank 0 (communications included).

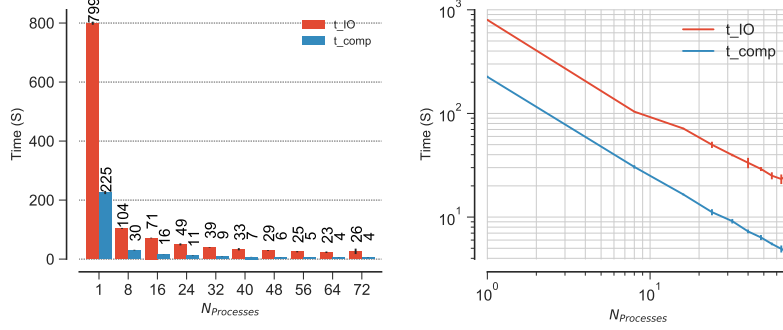


Figure 2: Scaling of the $t_{\text{compute_final}}$ and $t_{\text{I/O_final}}$ of the RMSD task with MPI.

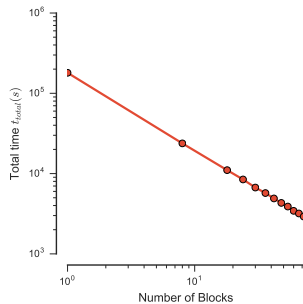
Hardware

We did not discern any specific patterns that could be traced to the underlying hardware. Stragglers were observed on *SDSC Comet*, *TACC Stampede* and *TACC Data Analytics System Wrangler* (data not shown). There was also no clear pattern in which certain MPI ranks would always be a straggler and we could also not trace stragglers to specific cores or nodes (or at least our data did not reveal an obvious pattern). Therefore, the phenomenon of stragglers in the RMSD test appears to be independent from the underlying hardware.

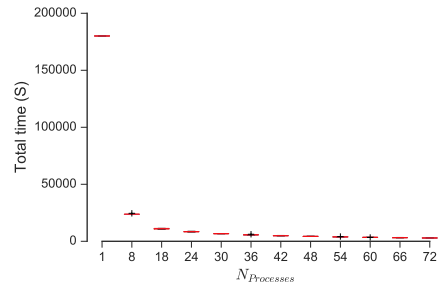
5.1. Dihedral Featurization Benchmarks

We briefly tested a much larger computational workload ($t_{\text{compute_per-frame}} = 40$ ms, $t_{\text{IO_per-frame}} = 0.4$ ms, thus $t_{\text{compute_final}}/t_{\text{I/O_final}} \approx 100$), namely dihedral featurization on *Comet* with Infiniband and Lustre file system.

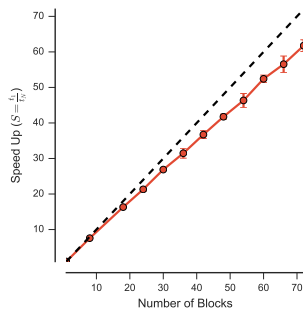
The system scales linearly and close to ideal (Figure 3). Although, there is communication of large result arrays, which is costly for multiple ranks, the speed-up curve (Eq. 1) in Figure 3c demonstrates very good scaling with the number of cores (up to 72 cores on 3 nodes). The reason is that the communication cost (for *MPI.Gather()*-lines 36-44 in 2) decreases with increasing the number of cores because the result array size that has to be communicated also decreases (Figure 4). Based on Figure 4, communication scales fairly well with the number of processes. This can be attributed to larger array sizes compared to the RMSD task and according to Dalcín et al. [5] the overhead of the



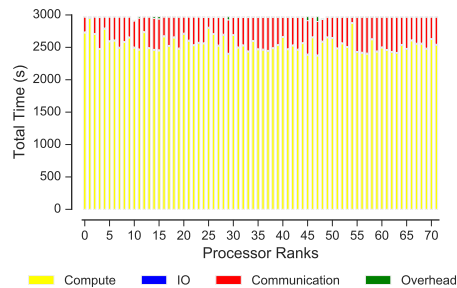
(a) Scaling total



(b) Total job execution time along with the mean and standard deviations across 5 repeats.



(c) Speed-up

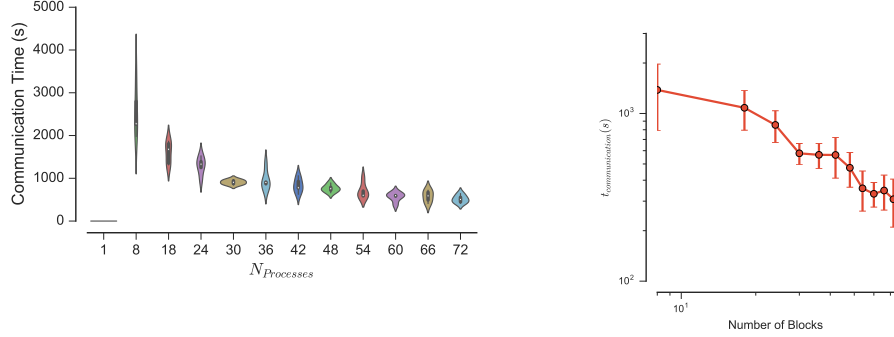


(d) time per MPI rank for a typical run (note, IO is almost too small to be visible)

Figure 3: Performance for the **dihedral featurization** workload, which is compute-bound $t_{\text{compute_final}}/t_{\text{I/O_final}} \approx 100$, when *communications are included*.

mpi4py package decreases as the array size to be communicated increases. The dihedral featurization workload has larger array size for all processor sizes (per task, a time series of feature vectors of size $N_b \times (213 \times 2 \times 2)$ when compared to the RMSD workload (per task a float array of length N_b) and therefore we are hypothesizing that the higher performance of *mpi4py* for larger array sizes has lead to better overall scaling. In addition, for higher computational workloads the competition over accessing the file is less severe as compared to lower computational workloads.

Overall, increasing the computational workload over I/O improves scaling. For large compute-bound workloads such as the dihedral featurization task, stragglers are eliminated and nearly ideal strong scaling is achieved. The fact



(a) Communication time distribution for different number of processes (shown as violin plots [14] with kernel density estimates as implemented in *seaborn*); the white dot indicates the median.

(b) Scaling communication time (mean and standard deviation)

Figure 4: Comparison of communication cost for different number of processes over 5 repeats for the **dihedral featurization** workload (with *communications included*).

that linear scaling is possible, even with expensive communications, makes parallelization a valuable strategy to reduce the total time to solution for large computational workloads. In a real-world application to one of our existing data sets on local workstations with Gigabit interconnect and Network File System (NFS) (using the Dask parallel library instead of MPI), analysis time was reduced from more than a week to a few hours (data not shown).

5.2. Effect of $t_{\text{compute_final}}/t_{\text{I/O_final}}$ on Performance

The RMSD task turned out to be I/O bound, i.e.,

$$\frac{t_{\text{compute_final}}}{t_{\text{I/O_final}}} \ll 1.$$

and we were not able to achieve good scaling above a single node. However, Dihedral featurization turned out to be compute bound and we were able to achieve near ideal scaling. We therefore, hypothesized that decreasing the relative I/O load with respect to compute load would also reduce the stragglers. We therefore increased the computational load so that the work became compute bound, i.e.,

$$\frac{t_{\text{compute_final}}}{t_{\text{I/O_final}}} \gg 1.$$

i.e., now processes are not constantly performing I/O and instead, I/O is interleaved with longer periods of computation. In order to artificially increase the computational load we repeated the same RMSD calculation (line 10, algorithm 1) 40, 70 and 100 times in a loop respectively.

315 5.2.1. Increased workload (RMSD)

The RMSD workload was artificially increased forty-fold, seventy-fold, and hundred-fold and we measured performance as before. Figure 5 shows the effect of $t_{\text{compute_final}}/t_{\text{I/O_final}}$ ratio on performance. On average, each rank took $N_b \times t_{\text{I/O_final}}$ (where $N_b = N_{\text{frames}}/N$ is the number of frames per trajectory block, i.e., the number of frames processed by each MPI rank for N processes) for I/O, 320 $X \times N_b \times t_{\text{compute_final}}$ for the $X \times$ RMSD computation.

As the $t_{\text{compute_final}}/t_{\text{I/O_final}}$ ratio increases, speed-up and performance improves and show overall better scaling than the I/O-bound workload, i.e. $1 \times$ RMSD (Figure 5a). When $t_{\text{compute_final}}/t_{\text{I/O_final}}$ ratio increases, the RMSD calculation consistently scales up to larger numbers of cores ($N = 56$ for $70 \times$ 325 RMSD). Figures 5b and 5c shows the improvement in performance more clearly. In fact, as the $t_{\text{compute_final}}/t_{\text{I/O_final}}$ ratio increases, the values of speed-up and efficiency get closer to their ideal value for each number of processor counts.

Even for moderately compute-bound workloads such as the $40 \times$ and $70 \times$ 330 RMSD tasks, increasing the computational workload over I/O reduced the impact of stragglers even though they still contribute to large variations in timing across different ranks and thus to somewhat erratic scaling.

Given the results for Dihedral featurization and RMSD algorithms (Algorithms 2, and 1) and $X \times$ RMSD (Figure 5) **we hypothesize that MPI competes with Lustre on the same network interface, which would explain** 335 **why communication appears to be primarily a problem in the pres-**

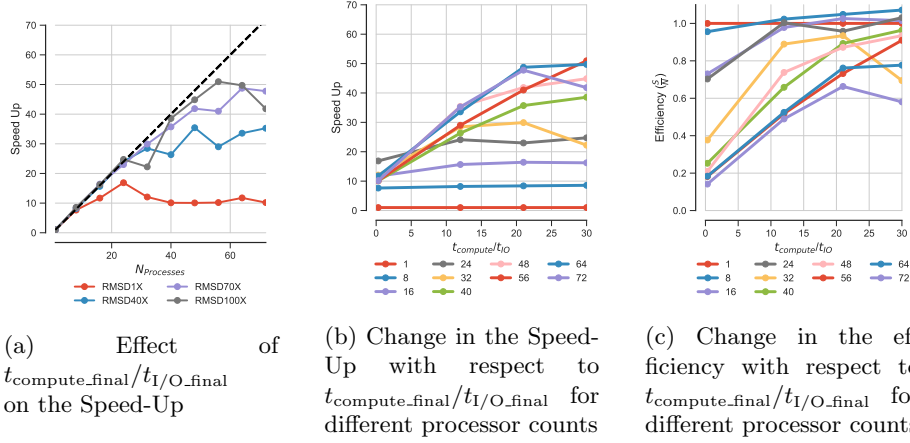


Figure 5: Performance change of the RMSD task with MPI with different $t_{\text{compute_final}}/t_{\text{I/O_final}}$ ratios. We tested performance for $t_{\text{compute_final}}/t_{\text{I/O_final}}$ ratios of 0.3, 12, 21, 30 which correspond to 1× RMSD, 40× RMSD, 70× RMSD, and 100× RMSD respectively (communication is included)

ence of I/O when $t_{\text{compute_final}}/t_{\text{I/O_final}}$ is small. In fact, decreasing the I/O load relative to the compute load should open up the network for communication.

5.3. Communication Cost and Application of Global Array

As discussed in the previous sections, 1c, for small $t_{\text{compute_final}}/t_{\text{I/O_final}}$ communication acts as the scalability bottleneck. In fact, when the processes communicate result arrays back to the master (rank 0) process, some processes take much longer as compared to other processes. Now we want to know what strategies can be used to avoid communication cost.

Algorithm 3 describes RMSD algorithm in combination with the global array. In this algorithm, we use global array instead of message passage paradigm to see if we can reduce communication cost. Given the speed up plots (Figure 6b) and total time scaling (Figure 6a) global array improves strong scaling performance. Although communication time has significantly decreased using global array (compare Figure 6c to Figure 1c), the existing variation in the dominant I/O part of the calculation would still prevent ideal scaling (Figure 7). In fact, although communications were performed using global arrays, scaling is still far from ideal as a result of slow processes due to I/O variation. These slow

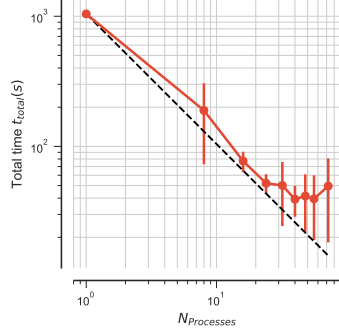
processes take about 50 s, which are slower than the mean execution time of all ranks, i.e. 17 s.

5.4. I/O Cost

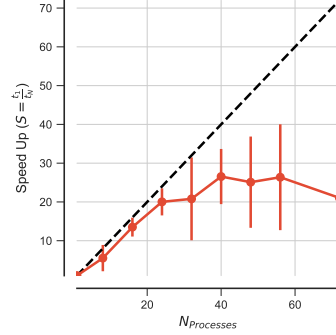
We showed previously that the I/O system can have a large effect on the parallel performance of the RMSD task [3], especially because the average time to perform the computation $t_{\text{compute_final}}$ (about 0.09 ms) is about three times smaller than the I/O time $t_{\text{I/O_final}}$ (about 0.3 ms) (Figures 2 and 1). In fact, poor I/O performance is responsible for the stragglers, and the question is “are stragglers waiting for file access?”. Due to the large file size and memory limit, processes are not able to load the whole trajectory into memory at once and as a result each process is only allowed to load one frame into memory at a time. The test trajectory has about 2,512,200 frames in total and as a result there will be 2,512,200 file access requests. Thus, when the compute time is small with respect to I/O, then I/O can be a major issue as we also see in our results (Figures 2 and 1). Read throughput might be limited by the available bandwidth on the Infini-band network interface that serves the Lustre file system and access to files might be throttled. In fact, we need to come up with ways and strategies to avoid the competition over file access across different ranks when $t_{\text{compute_final}}/t_{\text{I/O_final}}$ ratio is small. To this aim, we experimented two different ways for reducing I/O cost and examined their effect on the performance. These two ways include: Splitting the trajectory file into as many segments as number of processes and MPI-based Parallel HDF5. We discuss these two approaches in detail in the following sections.

5.4.1. Splitting the Trajectories

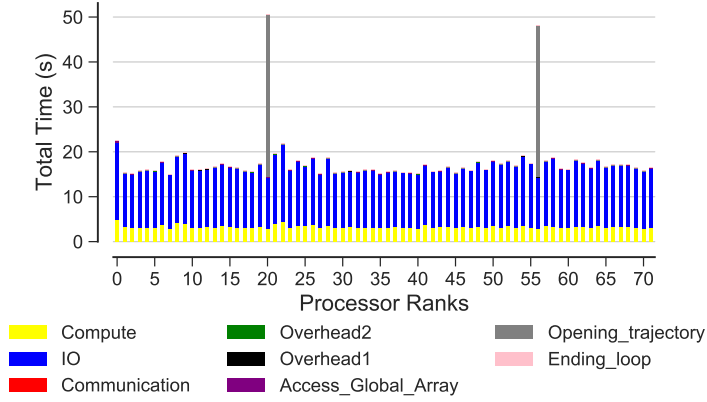
In all the previous benchmarks all processes were using a shared trajectory file. In order to test our hypothesis that *I/O and communication compete over the network resources with small $t_{\text{compute_final}}/t_{\text{I/O_final}}$ ratio*, we splitted our trajectory file into as many trajectory segments as the number of processes. This means that if we have N processes, the trajectory file is splitted into N



(a) Scaling total



(b) Speed-up



(c) Compute $t_{\text{compute_final}}$, IO $t_{\text{I/O_final}}$, communication t_{comm} , ending the for loop $t_{\text{end_loop}}$, opening the trajectory $t_{\text{opening_trajectory}}$, and overheads $t_{\text{Overhead1}}$, $t_{\text{Overhead2}}$ per MPI rank (as described in methods).

Figure 6: Performance of the RMSD task with MPI using global array ($t_{\text{compute_final}}/t_{\text{I/O_final}} \approx 0.3$). Data are read from the file system (I/O included). All ranks update the global array and rank 0 accesses the whole RMSD array through the global memory address.

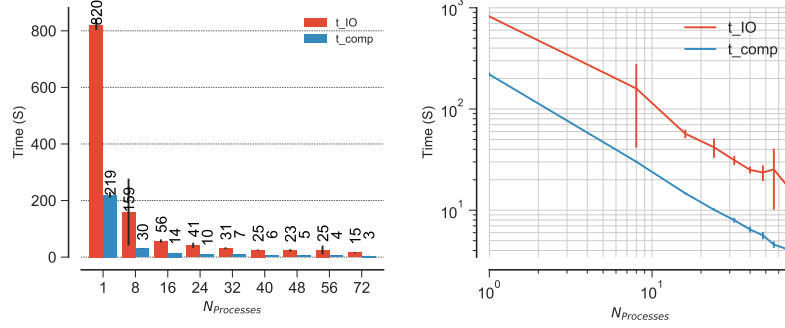


Figure 7: Scaling of the $t_{\text{compute_final}}$ and $t_{\text{I/O_final}}$ of the RMSD task with Global Array.

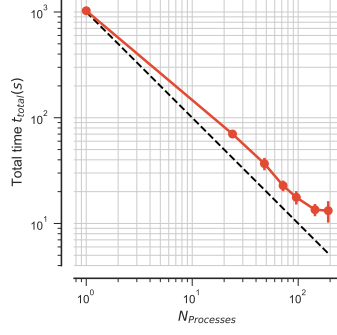
segments and each segment will have N_b frames in it. Through this approach,
 385 each process will have access to its own segment and there will be no competition
 over file accesses. For reference, the necessary time for splitting the trajectory
 file is given in Appendix Appendix A.

Performance without Global Array

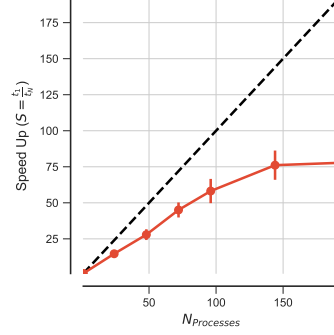
We ran a benchmark up to 8 nodes (192 cores) and, we observed rather better
 390 scaling behavior with efficiencies above 0.6 (Figure 8a and 8b) and the delay time
 for stragglers has also reduced from 65 to about 23 (Compare Figure 8c to 1c).
 However, the scaling is still far from ideal due to the communication. Although
 the delay due to communication is much smaller as compared to RMSD with
 a shared trajectory file (Compare Figure 8c to Figure 1c), it is still delaying
 395 several processes and as a result leads to longer job completion time (Figure
 8c). These delayed tasks impact performance as well and hence the speed-up is
 not still close to ideal scaling (Figure 8b).

Performance using Global Array

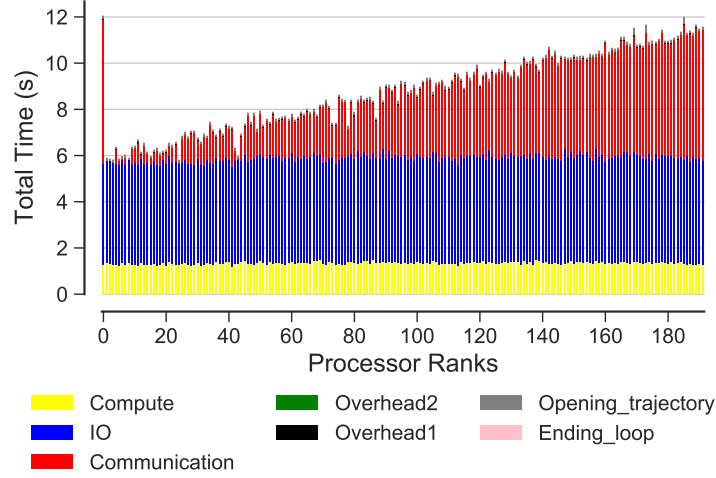
Previously, we showed that global array significantly reduces the communi-
 400 cation cost (Section 5.3). We want to see how the performance looks like if we
 split our trajectory file and take advantage of global array. Again, we ran our
 benchmark up to 8 nodes (192 cores) and, we observed near ideal scaling be-
 havior with efficiencies above 0.9 (Figure 10a and 10b) with no straggler tasks



(a) Scaling total



(b) Speed-up



(c) Compute $t_{compute_final}$, IO t_{I/O_final} , communication t_{comm} , ending the for loop t_{end_loop} , opening the trajectory $t_{opening_trajectory}$, and overheads $t_{Overhead1}$, $t_{Overhead2}$ per MPI rank (as described in methods).

Figure 8: Performance of the RMSD task with MPI using global array ($t_{compute_final}/t_{I/O_final} \approx 0.3$). Data are read from the file system (I/O included). All ranks update the global array and rank 0 accesses the whole RMSD array through the global memory address.

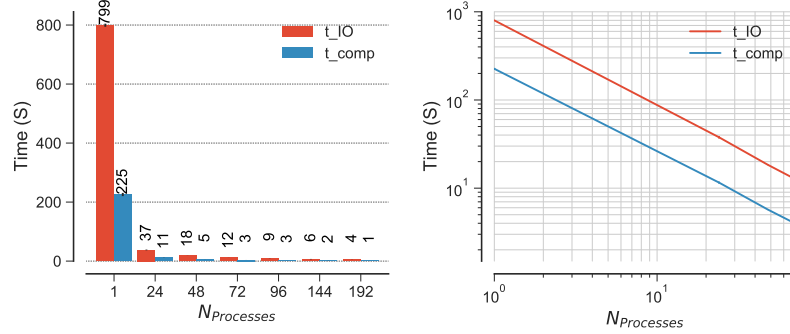


Figure 9: Scaling of the $t_{compute_final}$ and t_{I/O_final} of the RMSD task with Global Array.

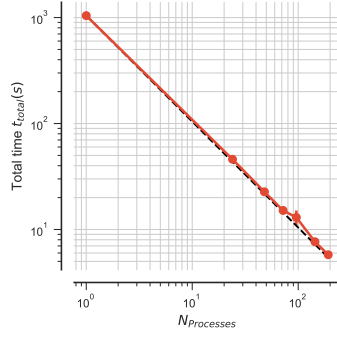
(Figure 10c). The present results show that contention for a file impacts the performance. The initial results with splitting the trajectory file suggests that there is in fact an effect, which possibly also interferes with the communications when $t_{compute_final}/t_{I/O_final} \ll 1$ (i.e. with a I/O bound workload).

5.4.2. MPI-based Parallel HDF5

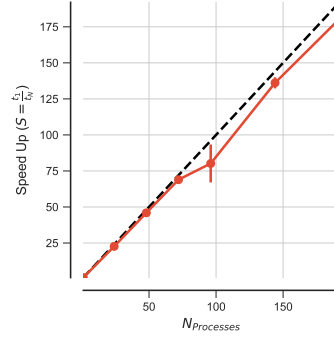
Another approach we examined to improve I/O scaling is MPI-based Parallel HDF5. We converted our XTC trajectory file into HDF5 format so that we can test the performance of parallel IO with HDF5 file format. The time it took to convert our XTC file with 2,512,200 frames into HDF5 format was about 5400 s in our local resources with network file system (NFS). Again, we ran our benchmark up to 8 nodes (192 cores) and, we observed near ideal scaling behavior with efficiencies above 0.8 (Figure 12a and 12b) with no straggler tasks (Figure 12c). When we split our trajectory, scaling is better as compared to that of parallel I/O (Compare Figure 12b to Figure 10b). However, both methods scale very well up to 8 nodes and have comparable performance.

6. Guidelines on the Parallel Analysis of Three Dimensional Time Series

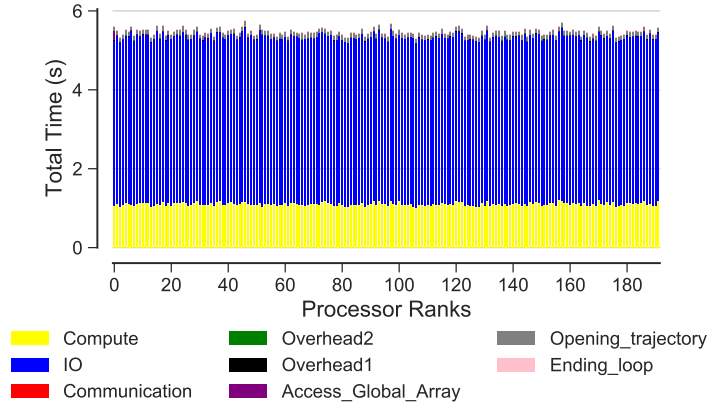
Parallel implementation of the three dimensional time series is performed in the following steps:



(a) Scaling total



(b) Speed-up



(c) Compute $t_{\text{compute_final}}$, IO $t_{\text{I/O_final}}$, communication t_{comm} , ending the for loop $t_{\text{end_loop}}$, opening the trajectory $t_{\text{opening_trajectory}}$, and overheads $t_{\text{Overhead1}}$, $t_{\text{Overhead2}}$ per MPI rank (as described in methods).

Figure 10: Performance of the RMSD task with MPI using global array ($t_{\text{compute_final}}/t_{\text{I/O_final}} \approx 0.3$). Data are read from the file system (I/O included). All ranks update the global array and rank 0 accesses the whole RMSD array through the global memory address.

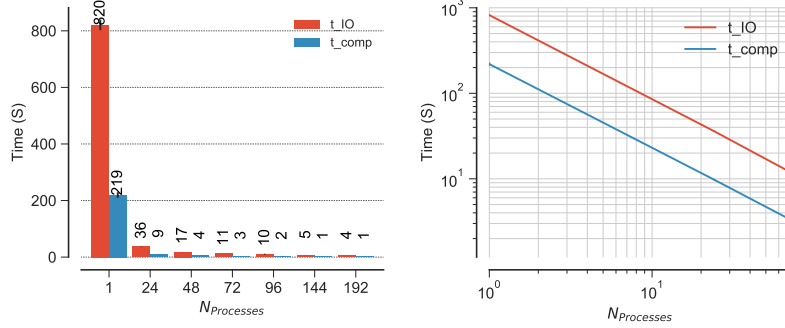


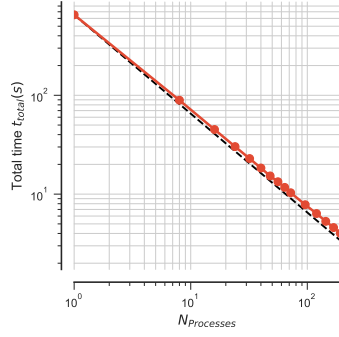
Figure 11: Scaling of the $t_{compute_final}$ and t_{I/O_final} of the RMSD task with Global Array.

Step 1 Calculate the value of $t_{compute_final}/t_{I/O_final}$ to see whether the task is compute bound ($\frac{t_{compute_final}}{t_{I/O_final}} \gg 1$) or IO bound ($\frac{t_{compute_final}}{t_{I/O_final}} \ll 1$). As discussed in Section 5.2 for I/O bound problems both communication and I/O will be a problem and the performance of the task will be affected by the straggler tasks which delay job completion time.

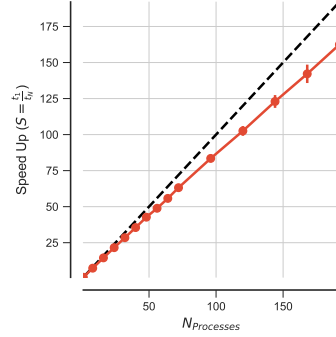
Step 2 For $\frac{t_{compute_final}}{t_{I/O_final}} \geq 100$ the task is compute bound and the task will scale very well as we showed in Section 5.1. However, if the size of the data to be communicated to rank 0 using the blocking collective communication ($MPI.Gather()$) is small, one might consider using global arrays to achieve near ideal scaling behavior (Section 5.3). In fact the overhead of *mpi4py* is large with respect to C for small array size. Application of Global array is useful in the sense that it replaces message-passing interface with a distributed shared array where its blocks will be updated by the associated rank in the communication domain (Algorithm 3).

Step 3 For $\frac{t_{compute_final}}{t_{I/O_final}} \leq 100$ the task is I/O bound and then one need to take the following steps:

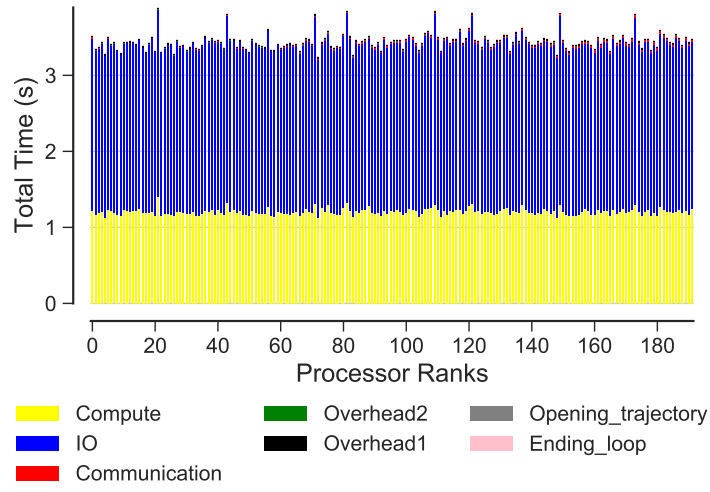
- If there is access to HDF5 format the recommended way will be to use MPI-based Parallel HDF5 (Section 5.4.2). Since converting the XTC file to HDF5 is expensive if the trajectory file formats are not in HDF5 form then one might prefer to split the trajectories.



(a) Scaling total



(b) Speed-up



(c) Compute $t_{\text{compute_final}}$, IO $t_{\text{I/O_final}}$, communication t_{comm} , ending the for loop $t_{\text{end_loop}}$, opening the trajectory $t_{\text{opening_trajectory}}$, and overheads $t_{\text{Overhead1}}$, $t_{\text{Overhead2}}$ per MPI rank (as described in methods).

Figure 12: Performance of the RMSD task with MPI-based parallel HDF5 ($t_{\text{compute_final}}/t_{\text{I/O_final}} \approx 0.3$). Data are read from the file system from a shared HDF5 file instead of XTC format (Independent I/O).

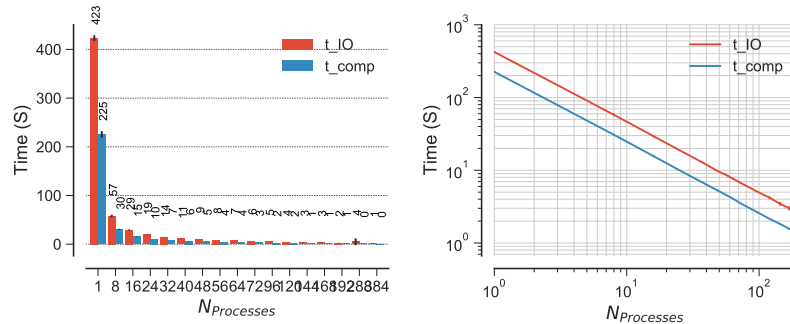


Figure 13: Scaling of the $t_{compute_final}$ and t_{I/O_final} of the RMSD task with MPI-based parallel HDF5 (Independent I/O).

- If there is not access to HDF5, the trajectory file should be splitted into as many trajectory segments as the number of processes. Splitting the trajectories is fast and does not take much time (Appendix Appendix A).
- The appropriate parallel implementation along with *Global Array* should be used on the trajectory segments (Section 5.4.1) to achieve near ideal scaling.

7. Conclusion

There are currently many freely available libraries for the analysis and processing of three-dimensional time series. However, dramatic increases in the size of trajectories combined with the serial nature of these libraries necessitates use of state of the art high performance computing tools for rapid analysis of these time series.

We have been able to identify the root cause for stragglers in our MPI test case and our data suggest a **new specific hypothesis**. We tested our benchmark on RMSD (I/O bound) and Dihedral featurization (compute bound) algorithms in *MDAnalysis*. Both communication and I/O appeared to be the scalability bottleneck for our RMSD benchmark test case when using a shared file.

In fact, for I/O-bound workload, *stragglers are due to the competition between MPI and the Lustre file system on the shared Infini-band interconnect.* This hypothesis appears to be consistent with the observation that for larger
465 number of process counts, communication is primarily a problem in the presence of many I/O requests produced by I/O-bound workloads. In fact, communication time t_{comm} , i.e., the `mpi4py.MPI.COMM_WORLD.Gather()` step, could take much longer for stragglers than for “normal” MPI ranks when I/O has to be performed through a shared trajectory file (Figure 1c).

470 The ratio between compute load and I/O load appeared to be crucial as well. For sufficiently large per-frame workloads, close to ideal scaling was achievable (Figure 3). Additionally, the effect of communication was less pronounced when the work became more compute-bound. This is because with compute-bound tasks there is less competition over accessing the shared trajectory file.

475 For I/O bound tasks we needed to come up with solution to overcome stragglers. We were able to achieve much better performance in our RMSD benchmark when we used global array toolkit instead of message-passing interface for communication. Using global array, we did not observe any delayed task due to communication (Figure 6) and it significantly reduces the communication cost.

480 However, reducing communication cost was not enough for achieving near ideal scaling. We were able to improve I/O through splitting the shared trajectory file and parallel I/O (Figures 8 and 12). In both cases we were able to achieve near ideal scaling. With splitting the trajectories, effect of communication is still apparent on the performance; however we could tackle this problem
485 using global array toolkit (Compare Figure 8 to Figure 10).

All the above strategies, provides the bio-molecular simulation community the means to perform a wide variety of parallel analyses on data generated from computational simulations. The guidelines provided in the present study, help people to tackle their problem depending on the workload being I/O bound
490 or compute bound. The analysis indicates that splitting the trajectories in combination with global array or parallel I/O will make it feasible to run a I/O bound task on scalable computers up to 8 nodes and achieve near ideal scaling

behavior.

References

- 495 1. Gowers RJ, Linke M, Barnoud J, Reddy TJE, Melo MN, Seyler SL, et al.
MDAnalysis: A Python package for the rapid analysis of molecular dy-
namics simulations. In: Benthall S, Rostrup S, editors. Proceedings of
the 15th Python in Science Conference. Austin, TX: SciPy; 2016, p. 102
–9. URL: <http://mdanalysis.org>.
- 500 2. Michaud-Agrawal N, Denning EJ, Woolf TB, Beckstein O. MDAnalysis:
A toolkit for the analysis of molecular dynamics simulations. J Comp
Chem 2011;32:2319–27. doi:10.1002/jcc.21787.
3. Khoshlessan M, Paraskevagos I, Jha S, Beckstein O. Parallel analysis in
MDAnalysis using the Dask parallel computing library. In: Katy Huff
505 , David Lippa , Dillon Niederhut , Pacer M, editors. Proceedings of the
16th Python in Science Conference. Austin, TX: SciPy; 2017, p. 64–72.
doi:10.25080/shinma-7f4c6e7-00a.
4. Rocklin M. Dask: Parallel computation with blocked algorithms and task
scheduling. In: Proceedings of the 14th Python in Science Conference.
510 130–136; 2015, URL: <https://github.com/dask/dask>.
5. Dalcín LD, Paz RR, Kler PA, Cosimo A. Parallel distributed computing
using python. Advances in Water Resources 2011;34(9):1124–39. doi:10.
1016/j.advwatres.2011.04.013; new Computational Methods and
Software Tools.
- 515 6. Dalcín L, Paz R, Storti M. MPI for python. Journal of Parallel and Dis-
tributed Computing 2005;65(9):1108–15. doi:10.1016/j.jpdc.2005.
03.010.
7. DAILY JA. Gain: Distributed array computation with python. Master’s
thesis; School of Electrical Engineering and Computer Science, WASH-
520 INGTON STATE UNIVERSITY; 2009.
8. Nieplocha J, Palmer B, Tipparaju V, Krishnan M, Trease H, Aprà E. Ad-

vances, applications and performance of the global arrays shared memory programming toolkit. *The International Journal of High Performance Computing Applications* 2006;20(2):203–31.

- 525 9. Collette A. In: *Python and HDF5*. 2014,.
10. Liu P, Agrafiotis DK, Theobald DL. Fast determination of the optimal rotational matrix for macromolecular superpositions. *J Comput Chem* 2010;31(7):1561–3. doi:10.1002/jcc.21439.
11. Theobald DL. Rapid calculation of RMSDs using a quaternion-based
530 characteristic polynomial. *Acta Crystallogr A* 2005;61(Pt 4):478–80. doi:10.1107/S0108767305015266.
12. Sittel F, Jain A, Stock G. Principal component analysis of molecular dynamics: on the use of cartesian vs. internal coordinates. *J Chem Phys* 2014;141(1):014111. doi:10.1063/1.4885338.
- 535 13. Seyler SL, Beckstein O. Sampling of large conformational transitions: Adenylate kinase as a testing ground. *Molec Simul* 2014;40(10–11):855–77. doi:10.1080/08927022.2014.919497.
14. Hintze JL, Nelson RD. Violin plots: A box plot-density trace synergism. *The American Statistician* 1998;52(2):181–4. URL:
540 <http://www.tandfonline.com/doi/abs/10.1080/00031305.1998.10480559>. doi:10.1080/00031305.1998.10480559. arXiv:<http://www.tandfonline.com/doi/pdf/10.1080/00031305.1998.10480559>.

Algorithm 2 Dihedral Featurization

Input: *mobile*: the desired atom groups to perform RMSD on them
start & *stop*: that tell which block of trajectory (frames) is assigned to each rank
topology & *trajectory*: files to read the data structure from
Output: Calculated Dihedral Angles

```
1: procedure angle2sincos(x)
2:   return [np.cos(x), np.sin(x)]
3: end procedure
4:
5: procedure residues_to_dihedrals(residues)
6:   for  $\forall res$  in residues do
7:     list( $\phi(res)$ ,  $\psi(res)$ )
8:   end for
9: end procedure
10:
11: procedure featurize_dihedrals(dihedrals)
12:   angles = [dihedral.value() for dihedral in dihedrals]
13:   return angle2sincos(angles)
14: end procedure
15:
16: procedure Block_Dihedral(index, topology, trajectory, xref0, start=None, stop=None,
    step=None)
17:   start0 = time.time()
18:   clone = mda.Universe(topology, trajectory)
19:   g = clone.atoms[index]
20:
21:   start1 = time.time()
22:   start0 = start1
23:   for  $\forall iframe, ts$  in enumerate(clone.trajectory[start : stop : step]) do
24:     start2 = time.time()
25:     Append in results featurize_dihedrals(dihedrals)
26:     t_comp[iframe] = time.time() - start2                                 $\triangleright$  Compute per frame
27:     t_IO[iframe] = start2 - start1                                          $\triangleright$  I/O per frame
28:     start1 = time.time()
29:   end for
30:   start3 = time.time()
31: end procedure
32:
33: start4 = time.time()
34: out = Block_Dihedral(index, topology, trajectory, xref0, start=start,
    stop=stop, step=1)
35:
36: start5 = time.time()
37: if rank == 0 then
38:   data1 = np.zeros([size*bsize, np.shape(out)[1]], dtype=float)
39: else
40:   data1 = None
41:   comm.Gather(out[0], data1, root=0)
42: end if
43:
44: start6 = time.time()
```

Algorithm 3 Global Array instead of Message-Passing Paradigm

Input: *mobile*: the desired atom groups to perform RMSD on them
bsize: Total number of frames assigned to each rank N_b
g_a: Initialized global array of ($bsize * size, 2$)
buf: Initialized buffer to store final calculated RMSD results of size ($bsize * size, 2$)
xref0: mobile group in the initial frame which will be considered as reference
start & *stop*: that tell which block of trajectory (frames) is assigned to each rank
topology & *trajectory*: files to read the data structure from
Output: Calculated RMSD arrays

```
1: bsize = int(np.ceil(mobile.universe.trajectory.nframes / float(size)))
2: g_a = ga.create(ga.CDBL, [bsize*size,2], "RMSD")
3: buf = np.zeros([bsize*size,2], dtype=float)
4:
5: start4 = time.time()
6: out = Block.RMSD(index, topology, trajectory, xref0, start=start, stop=stop,
  step=1)
7: start5 = time.time()
8:
9: ga.put(g_a, out[:, :], (start,0), (stop,2))
10:
11: start6 = time.time()
12: if rank == 0 then
13:     buf = ga.get(g_a, lo=None, hi=None)
14: end if
15:
16: start7 = time.time()
```

Number of trajectory segments	N_p used for writing the segments	time (s)
24	24	89.92
48	48	46.79
72	72	33.7
96	96	25.12
144	144	43.7
196	196	13.49

Table A.2: The wall-clock time spent for writing N_p trajectory segments using N_p processes using MPI on SDSC Comet

Package	Version
PHDF5	1.10.1
h5py	2.7.1
GA4py	1.0
Global Array	5.6.1
MDAnalysis	0.17.0

Table A.3: Version of the packages used in the present study

Appendix A. Appendix

Detailed timing for splitting the trajectories.

545 *Version of the libraries used for the present study.*